

Fast Electron Filamentation a broad survey of material and angular initial conditions

Contact: drb509@york.ac.uk

D. R. Blackman

*York Plasma Institute, Department of Physics,
University of York,
YO10 5DD, United Kingdom*

A.P.L. Robinson

*Central Laser Facility
STFC Rutherford Appleton Laboratory
Harwell Oxford
OX11 0QX, United Kingdom*

J. Pasley

*York Plasma Institute, Department of Physics,
University of York,
YO10 5DD, United Kingdom*

Abstract

The filamentation of laser driven fast electron currents through targets has been observed in several previous experiments. The aim of this investigation is to link some of the theory of filamentation to structures observed in magnetic field measurements in high power laser experiments. The hybrid code Zephyros is used to study the level of fast electron beam filamentation in simple targets made from a wide range of elements under differing laser intensities. Using the Lee-More resistivity model and the Thomas-Fermi ionisation model very little difference in the level of filamentation is found. Other simulations run to investigate the link between the transverse electron temperature and filamentation of fast electron beams revealed that, for low injection angular spread, filamentation is suppressed.

1 Introduction

The filamentation of fast electron beams inside a target are of considerable interest in fast ignition fusion schemes and proton acceleration and have been studied before in several letters (see ref. [2, 3, 4]). An experiment performed on the Vulcan Petawatt laser in late 2011 [1] showed a mapping of the magnetic field around the rear of a target where small micron scale perturbations were seen. Simulations were run using zephyros supporting the idea that the perturbations were caused by filamentary electron beams. These filaments have been studied before in several letters (see ref. [2, 3, 4]). The mechanism for producing these filamented beams has also been a subject of discussion with some linking it to the Beam Weibel instability caused by large magnetic and electrical fields within the material [5]. These electrical and magnetic field are caused by the propagation of the fast electron beams through the target [6].

To explain the dynamics leading to these filaments

a linearised fluid model of fast electron is used as in ref. [7]. The momentum equation obtained using the method described in the paper is:

$$\frac{\partial u_{y,1}}{\partial t} = \frac{eu_{x,0}B_z}{\gamma m_e} - \frac{T_{f,\perp}}{\gamma m_e} \frac{\partial n_1}{\partial y} \quad (1)$$

Where u is the flow velocity of the fast electron, n being the number density, γ being the relativistic correction, and B being the local magnetic field. By taking the density (and therefore current) perturbations to be sinusoidal, the velocity (and therefore magnetic field) must be 90 out of phase, giving:

$$n_1 = n_{f_0} N \cos(ky) \quad (2)$$

$$j_x = eu_{x_0} n_{f_0} N \cos(ky) \quad (3)$$

$$u_{y_1} = u \sin(ky) \quad (4)$$

$$B_z = B \sin(ky) \quad (5)$$

The following solution to the momentum equation can be obtained (the full derivation can be seen in the paper [7] and [8]):

$$\ddot{N} + \beta \dot{N} - \alpha N = 0 \quad (6)$$

The last coefficient α is a growth term associated with the resistivity of the material. β is related to the transverse fast electron temperature $T_{f,\perp}$, which is essentially a measure of the *local* angular spread of the fast electron beam.

$$\beta = \frac{k_p^2 T_{f,\perp}}{\gamma m_e} \quad (7)$$

With $k_p = \frac{2\pi}{\lambda}$, where λ is the length scale of the transverse density perturbations that might seed filaments (i.e. the width of the filaments when looking down the beam). Two different solutions to this ODE now present themselves. first of these is where $\alpha \gg \beta$, gives the equation as before:

$$\ddot{N} = \alpha N \quad (8)$$

Given a solution of the form $N = Ae^{gt}$ and letting $g^3 = \alpha$ gives the relationship $N \propto e^{\alpha^{1/3}t}$, which is of the form of

an instability. The decay constant, g , only depends on one material property; the resistivity η .

$$g = \left[\frac{\eta(k e u_{x_0})^2 n_{f_0}}{\gamma m_e} \right]^{\frac{1}{3}} \quad (9)$$

This treatment is an approximation of the treatment shown in ref. [7] and it has been shown that the filamentation grows significantly even outside of the linear regime described. The dependence of this term on the resistivity points to a regime where the fast electron beam is unstable for increasing resistivity and more stable for decreasing resistivity. If there is a peak in the resistivity (as in the Lee-More model used in Zephyros) then the electron beam will remain relatively collimated until it hits an area of increasing resistivity, which equates to a region of the cold background electron fluid that is hotter than its surroundings. Once the surrounding cold electrons reach a threshold temperature the resistivity peaks and a region of falling resistivity occurs into which the fast electrons flow preferentially. This has the effect of splitting a larger beam into smaller beams that are collimated and continue through the target at an angle similar to that with which they were initially split off from the main beam.

In the other extreme where $\beta \gg \alpha$ we get this equation:

$$\ddot{N} = -\beta \dot{N} \quad (10)$$

If we use a similar solution to the one before:

$$N = A e^{gt} \quad (11)$$

Substitution back into eqn.10 yields $g^3 = -g\beta$ so $g = i\sqrt{\beta}$. This gives a solution of the form $N \propto e^{i\beta t}$, which if β is real gives an oscillatory rather than growing solution, meaning that the initial perturbations will simply ripple rather than grow in depth.

This leaves two predictions to test: the reduction of cold electron mean free path increasing the level of filamentation through the target, and a reduction in filamentation with smaller fast electron injection angles.

2 Simulations

Zephyros is a hybrid fast-electron code which uses a particle-in-cell model for the fast electron modelling whilst using a fluid for the background electrons to simulate the return current produced by large fast electron currents. In order to test both of the assertions set out in the introduction several simulations were run on aluminium targets. The targets had dimensions $200 \times 200 \times 50$ microns with the laser normal to the largest surface. An assumption of a glassy background ion spatial distribution is used, this implies both that

the mean free path of an electron is isotropic and that the movement of any ion from one site to another is not likely to effect the spatial distribution of the ion background. Given this it is reasonable to assume that any movement of ions is small compared with the scale lengths of this simulation and so a fixed ion background fluid can be used.

The Lee-More resistivity model and Thomas-Fermi ionisation model were used as supplied in Zephyros without modification. Magnetic fields were allowed to evolve and momentum exchange between the fast electrons and background electron fluid is also allowed.

The first set of simulations vary just the laser intensity starting at $5 \times 10^{19} Wcm^{-2}$ and continuing up to $5 \times 10^{20} Wcm^{-2}$. Figure 1 shows selected results from this survey, from these plots it is clear that there is an exact correlation between the temperature of the background electron fluid, the density of fast electrons and the resistivity of the target. In both intensity regimes the filaments appear to be around a few microns in diameter. The higher intensity simulations appear to have more filaments overall with some of the central filaments appearing to merge. The lower intensity simulations have a more even spread of filaments across the centre and gradually disperse towards the edge.

In the second set of simulations the effect of varying the material composition is explored, by changing the material the mean free path of the cold electrons can be altered. The resistivity and ionisation models vary with the Z, A and ion density of each element. The location of the peak in the Lee-More resistivity changes slightly (between 20 and 40eV) with increasing Z, slowly moving to higher temperatures. The importance of the peak location can be seen in the resistivity plots in fig. 1 where the resistivity is observed to rise up to the edge of the filament and then falls dramatically back down again towards the centre of the filament. The temperature however, rises continually to the centre of the filaments.

The subject of the final set of simulations is the investigation into the effect of varying the injection angle of the fast electrons upon filamentation. The Zephyros code injects electrons in a diffuse manner, i.e in each cell where the electrons are injected, the angular distribution is the same, so that when a sample is taken from any local area near the injection point the angular spread is relatively high. The injection angle specifies the maximum angular spread of the electrons: It is measured from the central axis, and the individual electrons have angles assigned to them by sampling from a uniform distribution of angles within the maximum.

When the injection angle is decreased the level of

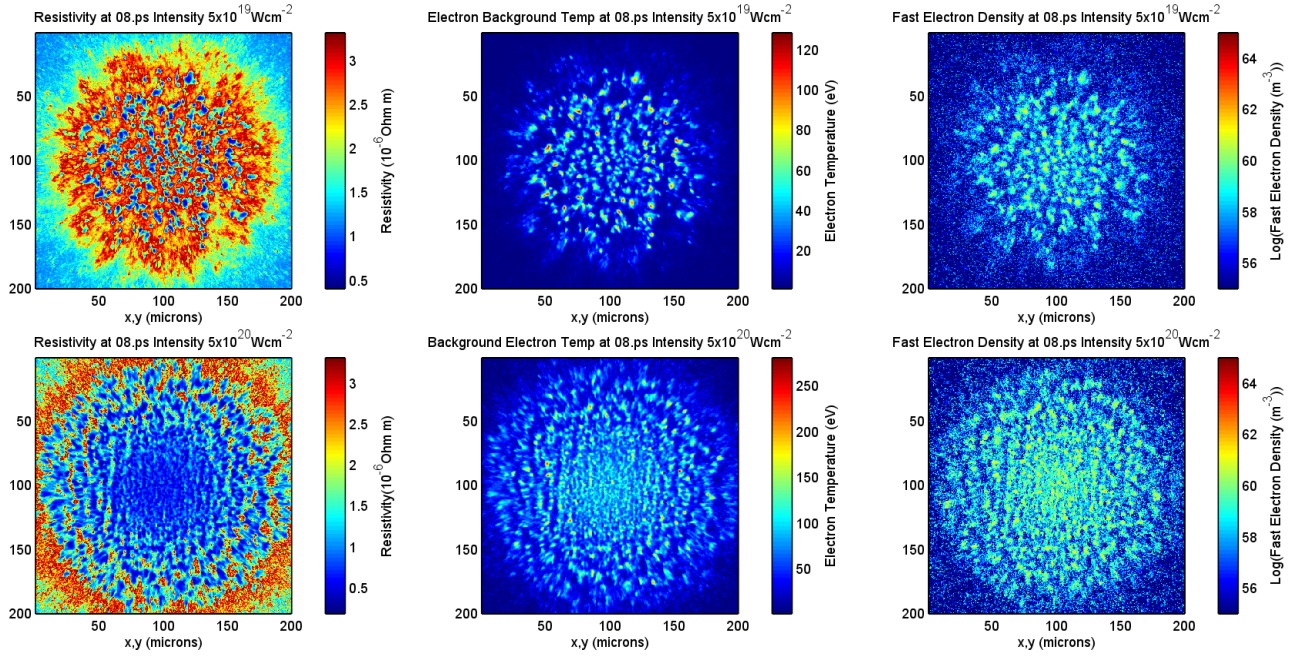


Figure 1: Plots showing resistivity, background electron temperature and fast electron density at the target rear, for two different intensities ($5 \times 10^{19} Wcm^{-2}$ & $5 \times 10^{20} Wcm^{-2}$) incident on a simulated Aluminium target. Both show a high degree of correlation across the measured parameters.

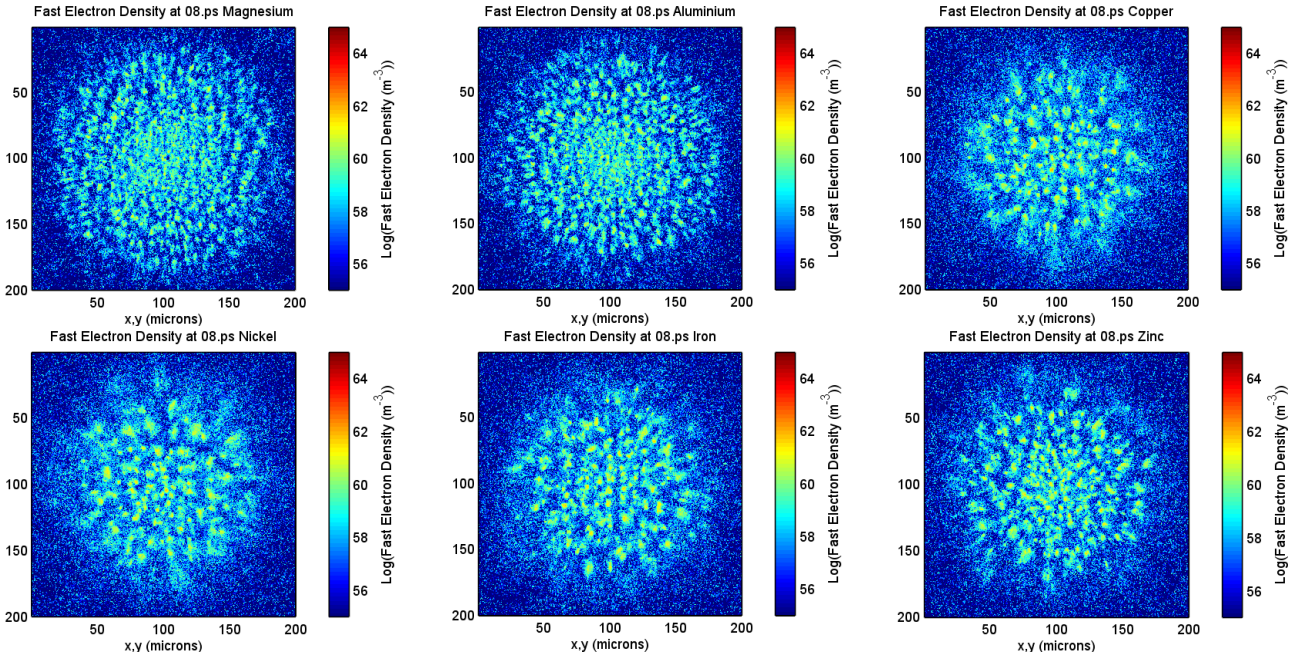


Figure 2: Plots showing the fast electron density at the target rear for the material scan at a laser intensity of ($2 \times 10^{20} Wcm^{-2}$). Some variation in the scale and distribution of the filaments is apparent with the filaments slowly increasing in areal scale with element Z.

filamentation dramatically decreases and a high degree of collimation of the fast electron beam is observed. If there is a wide divergence angle, far from the source of the electrons, the spread narrows quickly as most of the electrons need to have similar divergence angles to reach

similar locations. This means that for high injection divergence angles there is a decreasing transverse temperature with increasing distance from the source, i.e. β is reduced as you travel further into the target. Conversely if there is, initially, a narrow spread of

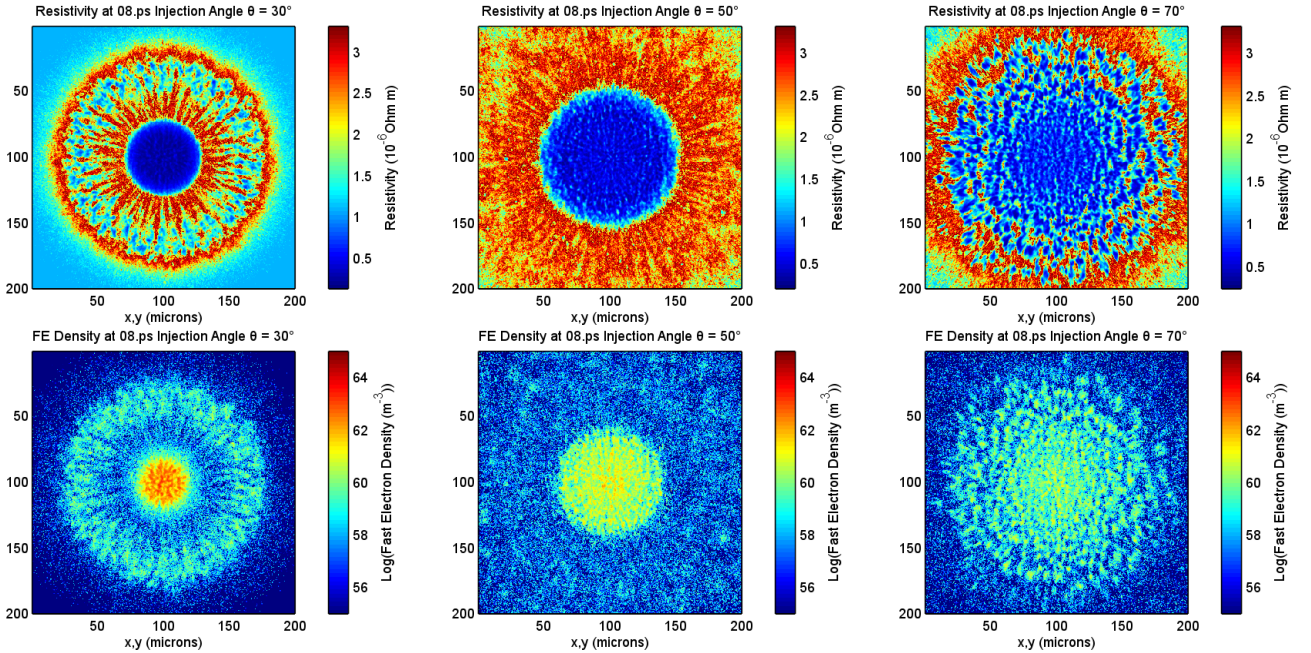


Figure 3: Resistivity and Fast Electron Density plots for three different fast electron injection angles, 30° , 50° and 70° . The low injection angle case shows a distinctive halo around the outside of a highly collimated central electron beam whilst higher angles show no such halo and increasing levels of filamentation. The Halo is due to reflusing electrons and is only visible after 0.6ps. These simulations were run at a laser intensity of $2 \times 10^{20} W cm^{-2}$.

injection angle then electrons further from the injection point are likely to sustain a similar angular spread further into the target. The persistence of a higher angular spread of electron velocities has the effect of suppressing filamentation growth.

3 Conclusion

The scan through laser intensity show that as the intensity of a shot increases fast electron beam filaments occur with similar diameters and with an overall increase in numbers.

The cold electron mean free path is only taken account of in Zephyros by the ionisation and resistivity models used, these models only vary with the type of material present in the target as does the cold electron mean free path. This reinforces the conclusion that if the diameter of the filaments is mainly dependant on the cold electron mean-free path then they should only change diameter significantly when the target material is changed. Materials with a smaller mean free path would then lead to higher resistivities at low temperatures resulting in a greater level of filamentation.

This difference in the diameter of the electron beam filamentation across materials is not very large and given how little the location of the peak in the Lee-More resistivity changes with mean free path it is not surprising that there is not a large difference in the diameter

of the filaments.

The lower level of filamentation with smaller divergence angle can be explained by the dependence of β on the *local* angular spread rather than on the *global* spread. This is taken into account in the β coefficient through the perpendicular temperature $T_{f,\perp}$, where a low temperature would indicate a narrow angular spread in fast electron velocities and a wider spread being a higher temperature (see [7] for an alternative explanation).

References

- [1] G. Chatterjee, P. Singh, A. Robinson, N. Booth, O. Culfa, R. Dance, L. Gizzi, R. Gray, J. Green, P. Koester, G. Kumar, K. Lancaster, J. Pasley, N. Woolsey, and P. Rajeev, “Direct High-resolution Mapping of Megagauss Magnetic Fields in Petawatt Laser-Solid Interactions,” *To Be Published*.
- [2] L. Gremillet, G. Bonnaud, and F. Amiranoff, “Filamented transport of laser-generated relativistic electrons penetrating a solid target,” *Physics of Plasmas*, vol. 9, no. 3, p. 941, 2002.
- [3] M. Coury, D. Carroll, and A. Robinson, “Injection and transport properties of fast electrons in ultrain-

- tense laser-solid interactions,” *Physics of . . .*, vol. 20, no. 4, p. 043104, 2013.
- [4] a. Bret, M.-C. Firpo, and C. Deutsch, “Characterization of the initial filamentation of a relativistic electron beam passing through a plasma,” *Physical review letters*, vol. 94, p. 115002, Mar. 2005.
- [5] J. Hill, M. Key, S. Hatchett, and R. Freeman, “Beam-Weibel filamentation instability in near-term and fast-ignition experiments,” *Physics of plasmas*, vol. 12, no. 8, p. 082304, 2005.
- [6] J. Davies, “Electric and magnetic field generation and target heating by laser-generated fast electrons,” *Physical Review E*, vol. 68, pp. 1–7, Nov. 2003.
- [7] A. P. L. Robinson, R. J. Kingham, C. P. Ridgers, and M. Sherlock, “Effect of transverse density modulations on fast electron transport in dense plasmas,” *Plasma Physics and Controlled Fusion*, vol. 50, p. 065019, June 2008.
- [8] A. P. L. Robinson, D. J. Strozzi, J. R. Davies, L. Gremillet, J. J. Honrubia, T. Johzaki, R. J. Kingham, M. Sherlock, and A. A. Solodov, “Theory of Fast Electron Transport for Fast Ignition,” p. 0, Apr. 2013.